DE GRUYTER OPEN Curved and Layer. Struct. 2014; 1:1–10

Research Article Open Access

S. Natarajan*, A.J.M. Ferreira, and Hung Nguyen-Xuan

Analysis of cross-ply laminated plates using isogeometric analysis and unified formulation

Abstract: In this paper, we study the static bending and free vibration of cross-ply laminated composite plates using sinusoidal deformation theory. The plate kinematics is based on the recently proposed Carrera Unified Formulation (CUF), and the field variables are discretized with the non-uniform rational B-splines within the framework of isogeometric analysis (IGA). The proposed approach allows the construction of higher-order smooth functions with less computational effort. Moreover, within the framework of IGA, the geometry is represented exactly by the Non-Uniform Rational B-Splines (NURBS) and the isoparametric concept is used to define the field variables. On the other hand, the CUF allows for a systematic study of two dimensional plate formulations. The combination of the IGA with the CUF allows for a very accurate prediction of the field variables. The static bending and free vibration of thin and moderately thick laminated plates are studied. The present approach also suffers from shear locking when lower order functions are employed and shear locking is suppressed by introducing a modification factor. The effectiveness of the formulation is demonstrated through numerical examples.

Keywords: unified formulation; isogeometric analysis; non-uniform rational B-splines; shear locking; sinusoidal shear deformation theory

DOI 10.2478/cls-2014-0001
Received July 30, 2014 ; accepted September 3, 2014

***Corresponding Author: S. Natarajan:** Department of Mechanical Engineering, Indian Institute of Technology, Madras, Chennai - 600036, India,
Email: snatarajan@cardiffalumni.org.uk; snatarajan@iitm.ac.in
A.J.M. Ferreira: Faculdade de Engenharia da Universidade do Porto, Porto, Portugal
and Department of Mathematics, Faculty of Science, King Abdulaziz University, P.O. Box 80203, Jeddah 21589, Saudi Arabia
Hung Nguyen-Xuan: Department of Mechanics, Faculty of Mathematics and Computer Science, University of Science, HCMC, Vietnam

1 Introduction

The need for high strength-to-weight and high stiffness-to-weight ratio materials has led to the development of laminated composite materials. Typical laminated composites consist of layers of fibrous composite materials, which are combined to provide required engineering properties, such as in-plane stiffness, bending stiffness and coefficient of thermal expansion. This class of material has seen increasing utilization in structural elements, because of the possibility to tailor the properties to optimize the structural response. Some of the advantages exhibited by composite over alloys are light weight, reduced corrosion, reduced noise generation, lack of magnetic signature and shape adaptability. Moreover, by changing the orientation of the fibre between the laminae various coupling effects can be achieved, such as extension-shear, bend-twist and bend-extension. In the literature, different approaches have been employed to study the response of such laminated composite plates, ranging from complete 3D analysis to two-dimensional theories. Recently, a formulation based on three-dimensional consistency is being investigated [1, 2]. The main advantage of such a formulation is that it does not suffer from the shear locking syndrome and the through-thickness behaviour is represented analytically, whilst the in-plane behaviour can be described by any displacement-based formulations. However, in this paper, we restrict ourselves to conventional two dimensional plate theories. A brief overview of the development of different plate theories is given in [3, 4]. The various two dimensional plate theories can be further classified into three different approaches: (a) equivalent single layer theories [5], (b) discrete layer theories [6] and (c) mixed plate theory [7]. Among these, the equivalent single layer (ESL) theories, viz., the first order shear deformation theory [8], the second and the higher order accurate theory [5, 9] are the most popular theories employed to describe the plate kinematics. Although the plate kinematics can be described by various aforementioned theories, a systematic study on the influence of various theories on the structural response of laminated plates could be computationally intensive. Thanks to the recent derivation of a series of axiomatic approaches by Carrera [10], called the Carrera Unified Formulation [11], for the general description of two-dimensional formulations for multilayered plates and shells. With this unified formulation, it is possible to implement in a single software a series of hierarchical formulations, thus affording a systematic assessment of different theories, ranging from simple equivalent single layer models up to higher order layerwise descriptions. Ferreira *et al.*, [12, 13] studied the static and dynamic response of isotropic and cross-ply laminated composites by employing the unified formulation and the differential quadrature method.

Existing approaches in the literature to study plate and shell structures made up of laminated composites include the finite difference method [14], the singular convolution method [15], the finite element method based on Lagrange basis functions [16], non-uniform rational B splines (NURBS) [17], meshfree methods [18, 19] or the differential quadrature method [20, 21]. Not only do these approaches suffer from shear locking when applied to thin plates, these techniques do not provide a single platform to test the performance of various theories. Recent interest in the unified formulation has led to the development of discrete models such as those based on the finite element method [22, 23], and more recently, meshless methods [19]. Nevertheless, even with the unified framework, there is an important shortcoming when applied to thin plates. With lower order basis functions within the finite element framework, the formulation suffers from shear locking. Intensive research over the past decades has led to the development of robust methods to suppress the shear locking syndrome. These includes: (a) reduced integration [24]; (b) use of the assumed strain method [25]; (c) using field redistributed shape functions [26]; (d) the mixed interpolation tensorial components (MITC) technique with strain smoothing [27] and (e) very recently, the twist Kirchhoff plate element [28].

1.1 Objective

The main objective of this manuscript is to investigate the potential application of the NURBS-based isogeometric finite element method within the Carrera Unified Formulation (CUF) to study the global response of cross-ply laminated composites. The present formulation also suffers from shear locking when lower order basis functions are applied to thin plates. To address the shear locking problem with lower-order NURBS elements for plates, the introduction of a stabilization technique for shear locking has been studied [29]. The other approach to suppress shear locking is to employ higher order basis functions [30]. In this study, to alleviate shear locking, a simple modification is made to the shear term when lower order NURBS basis functions are used. However, the draw back of this approach is that the shear correction factor becomes problem dependent. The influence of various parameters, viz., the ply thickness, the ply orientation, the plate geometry, the material properties and the boundary conditions on the global response is studied numerically.

1.2 Outline

The paper commences with a brief discussion on the unified formulation for plates and the description of spatial discretization. Section 3 describes the isogeometric approach employed in this study, followed by a technique to address shear locking when lower order NURBS functions are used to discretize the field variables. The efficiency of the present formulation, numerical results and parametric studies are presented in Section 4, followed by concluding remarks in the last section.

2 Carrera Unified Formulation

2.1 Basis of the CUF

Let us consider a laminated plate composed of perfectly bonded layers with coordinates x, y along the in-plane directions and z along the thickness direction of the whole plate, while z_k is the thickness of the k^{th} layer. The CUF is a useful tool to implement a large number of two-dimensional models with the description at the layer level as the starting point. By following the axiomatic modelling approach, the displacements $\mathbf{u}(x, y, z) = (u(x, y, z), v(x, y, z), w(x, y, z))$ are written according to the general expansion as:

$$\mathbf{u}(x, y, z) = \sum_{\tau=0}^{N} F_\tau(z)\mathbf{u}_\tau(x, y) \tag{1}$$

where $F(z)$ are known functions to model the thickness distribution of the unknowns and N is the order of the expansion assumed for the through-thickness behaviour. By varying the free parameter N, a *hierarchical* series of two-dimensional models is obtained. The strains are related to the displacement field via the geometrical relations:

$$\begin{aligned} \boldsymbol{\varepsilon}_{pG} &= \begin{bmatrix} \varepsilon_{xx} & \varepsilon_{yy} & \gamma_{xy} \end{bmatrix}^{\mathrm{T}} = \mathbf{D}_p \mathbf{u} \\ \boldsymbol{\varepsilon}_{nG} &= \begin{bmatrix} \gamma_{xz} & \gamma_{yz} & \varepsilon_{zz} \end{bmatrix}^{\mathrm{T}} = (\mathbf{D}_{np} + \mathbf{D}_{nz})\,\mathbf{u} \end{aligned} \tag{2}$$

where the subscript G indicates the geometrical equations, and $\mathbf{D}_p$, $\mathbf{D}_{np}$ and $\mathbf{D}_{nz}$ are differential operators given by:

$$\mathbf{D}_p = \begin{bmatrix} \partial_x & 0 & 0 \\ 0 & \partial_y & 0 \\ \partial_y & \partial_x & 0 \end{bmatrix}, \quad \mathbf{D}_{np} = \begin{bmatrix} 0 & 0 & \partial_x \\ 0 & 0 & \partial_y \\ 0 & 0 & 0 \end{bmatrix},$$

$$\mathbf{D}_{nz} = \begin{bmatrix} \partial_z & 0 & 0 \\ 0 & \partial_z & 0 \\ 0 & 0 & \partial_z \end{bmatrix}. \tag{3}$$

The 3D constitutive equations are given as:

$$\begin{aligned} \boldsymbol{\sigma}_{pC} &= \mathbf{C}_{pp}\boldsymbol{\varepsilon}_{pG} + \mathbf{C}_{pn}\boldsymbol{\varepsilon}_{nG} \\ \boldsymbol{\sigma}_{nC} &= \mathbf{C}_{np}\boldsymbol{\varepsilon}_{pG} + \mathbf{C}_{nn}\boldsymbol{\varepsilon}_{nG} \end{aligned} \tag{4}$$

with

$$\mathbf{C}_{pp} = \begin{bmatrix} C_{11} & C_{12} & C_{16} \\ C_{12} & C_{22} & C_{26} \\ C_{16} & C_{26} & C_{66} \end{bmatrix} \quad \mathbf{C}_{pn} = \begin{bmatrix} 0 & 0 & C_{13} \\ 0 & 0 & C_{23} \\ 0 & 0 & C_{36} \end{bmatrix}$$
$$\mathbf{C}_{np} = \begin{bmatrix} 0 & 0 & 0 \\ 0 & 0 & 0 \\ C_{13} & C_{23} & C_{36} \end{bmatrix} \quad \mathbf{C}_{nn} = \begin{bmatrix} C_{55} & C_{45} & 0 \\ C_{45} & C_{44} & 0 \\ 0 & 0 & C_{33} \end{bmatrix} \tag{5}$$

where the subscript C indicates the constitutive equations. The *Principle of Virtual Displacements* (PVD) for a multilayered plate subjected to mechanical loads is written as:

$$\sum_{k=1}^{N_k} \int_{\Omega_k} \int_{A_k} \left\{ (\delta\boldsymbol{\varepsilon}_{pG}^k)^{\mathrm{T}} \boldsymbol{\sigma}_{pC}^k + (\delta\boldsymbol{\varepsilon}_{nG}^k)^{\mathrm{T}} \boldsymbol{\sigma}_{nC}^k \right\} \, \mathrm{d}\Omega_k \, \mathrm{d}z =$$
$$\sum_{k=1}^{N_k} \int_{\Omega_k} \int_{A_k} \rho^k \delta\mathbf{u}_s^{k^{\mathrm{T}}} \ddot{\mathbf{u}}^k \, \mathrm{d}\Omega_k \, \mathrm{d}z + \sum_{k=1}^{N_k} \delta\mathbf{L}_e^k \tag{6}$$

where ρ^k is the mass density of the k^{th} layer, Ω_k, A_k are the integration domains in the (x, y) and the z direction, respectively. Upon substituting the geometric relations (Equation (2)), the constitutive relations (Equation (4)) and the unified formulation into the PVD statement, we have:

$$\int_{\Omega_k}\int_{A_k} \left\{ \left(\mathbf{D}_p^k F_s \delta\mathbf{u}_s^k\right)^{\mathrm{T}} \left\{ \mathbf{C}_{pp}^k \mathbf{D}_p^k F_\tau \mathbf{u}_\tau^k + \mathbf{C}_{pn}^k (\mathbf{D}_{n\Omega}^k + \mathbf{D}_{nz}^k) F_\tau \mathbf{u}_\tau^k \right\} + \right.$$
$$\left. \left[(\mathbf{D}_{n\Omega}^k + \mathbf{D}_{nz}^k) f_x \delta\mathbf{u}_s^k)^{\mathrm{T}} (\mathbf{C}_{np}^k \mathbf{D}_p^k F_\tau \mathbf{u}_\tau^k + \mathbf{C}_{nn}^k (\mathbf{D}_{n\Omega}^k + \mathbf{D}_{nz}^k) F_\tau \mathbf{u}_\tau^k) \right] \right\} \times$$
$$\mathrm{d}\Omega_k \, \mathrm{d}z = \sum_{k=1}^{N_k} \int_{\Omega_k} \int_{A_k} \rho^k \delta\mathbf{u}_s^{k^{\mathrm{T}}} \ddot{\mathbf{u}}^k \, \mathrm{d}\Omega_k \, \mathrm{d}z + \sum_{k=1}^{N_k} \delta\mathbf{L}_e^k \tag{7}$$

After integration by parts, the governing equations for the plate are obtained:

$$\mathbf{K}_{uu}^{k\tau s} \mathbf{u}_\tau^k = \mathbf{P}_{u\tau}^k \tag{8}$$

and in the case of free vibrations, we have:

$$\mathbf{K}_{uu}^{k\tau s} \mathbf{u}_\tau^k = \mathbf{M}^{k\tau s} \ddot{\mathbf{u}}_\tau^k \tag{9}$$

where the fundamental nucleus $\mathbf{K}_{uu}^{k\tau s}$ is:

$$\mathbf{K}_{uu}^{k\tau s} = \Big[(-\mathbf{D}_p^k)^{\mathrm{T}} (\mathbf{C}_{pp}^k \mathbf{D}_p^k + \mathbf{C}_{pn}^k (\mathbf{D}_{n\Omega}^k + \mathbf{D}_{nz}) +$$
$$(-\mathbf{D}_{n\Omega}^k + \mathbf{D}_{nz}^k)^{\mathrm{T}} (\mathbf{C}_{np}^k \mathbf{D}_p^k + \mathbf{C}_{nn}^k (\mathbf{D}_{n\Omega}^k + \mathbf{D}_{nz}^k)) \Big] F_\tau F_s \tag{10}$$

and $\mathbf{M}^{k\tau s}$ is the fundamental nucleus for the inertial term given by:

$$M_{ij}^{k\tau s} = \begin{cases} \rho^k F_\tau F_s & \text{if} \quad i = j \\ 0 & \text{if} \quad i \neq j \end{cases} \tag{11}$$

where $\mathbf{P}_{u\tau}^k$ are variationally consistent loads with applied pressure. For a more detailed derivation and for the explicit form of the fundamental nuclei, interested readers are referred to [11, 31].

3 Non-uniform rational B-splines

In this study, the finite element approximation uses the NURBS basis functions. Here we give only a brief introduction to NURBS. More details on their use in FEM are given in [32]. The key ingredients in the construction of NURBS basis functions are: the knot vector (a non decreasing sequence of parameter values, $\xi_i \leq \xi_{i+1}$, $i = 0, 1, \cdots, m-1$), the control points P_i, the degree of the curve p and the weight associated with a control point, w. The ith B-spline basis function of degree p, denoted by $N_{i,p}$, is defined as:

$$N_{i,0}(\xi) = \begin{cases} 1 & \text{if } \xi_i \leq \xi \leq \xi_{i+1} \\ 0 & \text{else} \end{cases}$$
$$N_{i,p}(\xi) = \frac{\xi - \xi_i}{\xi_{i+p} - \xi_i} N_{i,p-1}(\xi) + \frac{\xi_{i+p+1} - \xi}{\xi_{i+p+1} - \xi_{i+1}} N_{i+1,p-1}(\xi) \tag{12}$$

The B-spline basis functions have the following properties: (i) non-negativity, (ii) partition of unity, $\sum_i N_{i,p} = 1$, (iii) interpolatory at the end points. As the same set of functions is also used to represent the geometry, the exact representation of the geometry is preserved. It should be noted that the continuity of the spline functions can be tailored to the needs of the problem. Also, the spline function has limited support. When employed to approximate the FE solution space, the resulting stiffness matrix has similar properties to the stiffness matrix computed by employing Lagrange shape functions. Given $n + 1$ control points $(\mathbf{P}_o, \mathbf{P}_1, \cdots, \mathbf{P}_n)$ and a knot vector $\Xi = \{\eta_o, \eta_1, \cdots, \eta_m\}$, the piecewise polynomial B-spline curve of degree p is defined as:

$$\mathbf{C}(\eta) = \sum_{i=0}^{n} \mathbf{P}_i N_{i,p}(\eta) \tag{13}$$

where $\mathbf{P}_i$ are the control points. A B-spline curve contains the following information: $n+1$ control points, $m+1$ knots and a degree p. It is noted that n, m and p must satisfy $m = n + p + 1$. The B-spline functions also provide a variety of refinement algorithms, which are essential when employing B-spline functions to discretize the unknown fields. The analogous h and p refinement can be done by the process of 'knot insertion' and 'order elevation'. The B-spline surfaces are defined by the tensor product of the basis functions in two parametric dimensions ξ and η with two knot vectors, one in each dimension:

$$\mathbf{C}(\xi, \eta) = \sum_{i=1}^{n} \sum_{j=1}^{m} N_{i,p}(\xi) M_{j,q}(\eta) \mathbf{P}_{i,j} \tag{14}$$

where $\mathbf{P}_{i,j}$ is the bidirectional control net and $N_{i,p}$ and $M_{j,q}$ are the B-spline basis functions defined on the knot vectors over an $m \times n$ net of control points $\mathbf{P}_{i,j}$. Despite the flexibility offered by the B-splines, they cannot exactly represent some shapes such as circles and ellipsoids. To improve this, non-uniform rational B-splines (NURBS) are constructed through rational functions of B-splines. The NURBS thus form the superset of B-splines. The key ingredients in the construction of NURBS basis functions are: the knot vector (a non decreasing sequence of parameter values, $\eta_i \leq \eta_{i+1}, i = 0, 1, \cdots, m-1$), the degree of the curve p and the weight associated to a control point, w. A p^{th} degree NURBS basis function is defined as follows:

$$R(\eta) = \frac{N_{i,p}(\eta) w_i}{W(\eta)} = \frac{N_{i,p}(\eta) w_i}{\sum_{i=0}^{n} N_{i,p}(\eta) w_i} \tag{15}$$

where w_i are the weights for the i^{th} basis function $N_{i,p}(\eta)$. Figure (1) shows the third order NURBS for an open knot vector $\Xi = \{0, 0, 0, 0, 1/3, 1/3, 1/3, 1/2, 2/3, 1, 1, 1, 1\}$.

The NURBS surface is then defined by:

$$\mathbf{R}(\xi, \eta) = \frac{\sum_{i=1}^{n} \sum_{j=1}^{m} N_{i,p}(\xi) M_{j,q}(\eta) \mathbf{P}_{i,j} w_i w_j}{w(\xi, \eta)} \tag{16}$$

where $w(\xi, \eta)$ is the weighting function. The displacement field, $\mathbf{u}_\tau(x, y)$ (see Equation (1)) within the control mesh is approximated by:

$$\mathbf{u}_\tau(x, y) = \mathbf{R}(\xi, \eta) \mathbf{q}_\tau(x, y), \tag{17}$$

where $\mathbf{q}_\tau(x, y)$ are the nodal variables and $\mathbf{R}(\xi, \eta)$ are the basis functions given by Equation (16). Similar to the finite element method based on Lagrange basis functions,

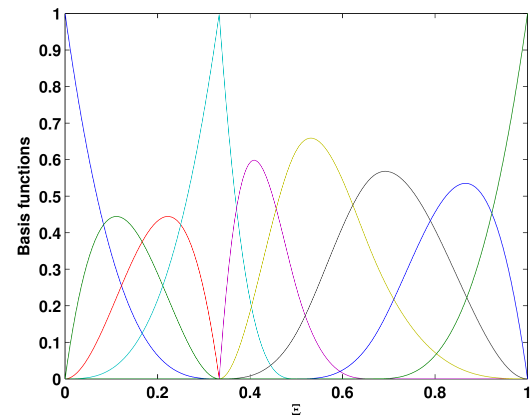

Figure 1: Non-uniform rational B-splines with an open knot vector, order of the curve = 3

locking appears when lower order NURBS basis functions are employed [30, 33], for example with quadratic, cubic and quartic elements[1]. One approach to alleviate the shear locking is to employ interpolation functions of order 5 or higher [30], but this inevitably increases the computational cost. A stabilization technique for several lower-order NURBS elements for plates was reported in [29]. In this paper, we adopt a stabilization technique proposed in [34] and later used in [33] to study the response of Reissner-Mindlin plates. In this approach, the material matrix related to shear terms are multiplied by the following factor:

$$\text{shearFactor} = \frac{h^2}{h^2 + \alpha^2 \ell^2} \tag{18}$$

where ℓ is the largest length of the edges of the NURBS element, and α is a positive constant limited to values $0.05 \leq \alpha \leq 0.15$. From numerical experiments of NURBS-based isogeometric plate elements it is found that setting $\alpha = 0.1$, yields reasonably accurate solutions.

4 Numerical Results

In this section, we present the static response and the natural frequencies of laminated composite plates using the combined IGA and CUF framework. In this study, we use a hybrid displacement assumption, where the in-plane displacements u and v are expressed as sinusoidal expan-

1 Linear NURBS basis functions are same as the linear Lagrange basis functions and are not discussed here. Approaches employed for Lagrange basis functions can readily be applied to NURBS basis functions with order 1

sions in the thickness direction, and the transverse displacement w is quadratic function in the thickness direction. We refer to this theory as SINUS-W2. The displacements are expressed as:

$$u(x, y, z, t) = u_o(x, y, t) + zu_1(x, y, t) + \sin\left(\frac{\pi z}{h}\right) u_2(x, y, t)$$
$$v(x, y, z, t) = v_o(x, y, t) + zv_1(x, y, t) + \sin\left(\frac{\pi z}{h}\right) v_2(x, y, t)$$
$$w(x, y, z, t) = w_o(x, y, t) + zw_1(x, y, t) + z^2 w_2(x, y, t) \tag{19}$$

where u_o, v_o and w_o are translations of a point at the mid-surface of the plate, w_2 is the higher order translation, and u_1, v_1, u_3 and v_3 denote rotations [35]. The effect of the plate aspect ratio, the ply angle and the ratio of Young's modulus E_1/E_2 on the static bending and free vibration is numerically studied.

4.1 Static bending

The static analysis is conducted for cross-ply laminated plates with three and four layers under the following sinusoidal load:

$$p_z(x, y) = P_o \sin\left(\frac{\pi x}{a}\right) \sin\left(\frac{\pi y}{a}\right) \tag{20}$$

where P_o is the amplitude of the mechanical load. The origin of the coordinate system is located at the lower left corner of the midplane. The physical quantities are non-dimensionalized by the following relations, unless otherwise mentioned:

$$\overline{w} = w(a/2, a/2, 0)\frac{100h^3 E_2}{P_o a^4};$$
$$\overline{\sigma}_{xx} = \sigma_{xx}(a/2, a/2, h/2)\frac{h^2}{P_o a^2};$$
$$\overline{\sigma}_{yy} = \sigma_{yy}(a/2, a/2, h/4)\frac{h^2}{P_o a^2};$$
$$\overline{\tau}_{xz} = \tau_{xz}(0, a/2, 0)\frac{h}{P_o a}. \tag{21}$$

Validation

Before proceeding with a detailed numerical study of the effect of various parameters on the global response of cross-ply laminated composites, the results from the proposed formulation are compared with available results pertaining to static bending of laminated plates. In this study, we consider three orders of NURBS basis functions, viz., quadratic, cubic and quartic. It is noted that, in this study, we do not consider first order NURBS basis functions. This is because, the first order NURBS basis functions are similar to the conventional bilinear shape functions. The performance of which is discussed in detail in [22, 23]. In this study, the results from the present formulation are denoted by Quadratic, Cubic and Quartic, which corresponds to the order of shape functions employed, referred to as p–refinement. Three different mesh discretizations, viz., 5×5, 7×7 and 9×9 are considered, called h–refinement. Table 1 shows the convergence of the central deflection and stresses of a simply supported cross-ply laminated square plate. It can be seen that with both h– and p–refinement, the results from the present formulation converge, and that highly accurate results are obtained from the present formulation even with a coarse mesh. A comparison with other approaches and an elasticity solution is given in Table 2.

Table 1: Convergence of the central deflection $\overline{w} = w(a/2, a/2, 0)\frac{100E_2h^3}{Pa^4}$ of a simply supported cross-ply laminated square plate [0°/90°/90°/0°] with $E_1 = 25E_2$, $G_{12} = G_{13} = 0.5E_2$, $G_{23} = 0.2E_2$, ν_{12} =0.25.

	Method	Meshes		
		5×5	7×7	9×9
$\overline{w}$	Quadratic	1.9207	1.9100	1.9058
	Cubic	1.9076	1.9038	1.9021
	Quartic	1.9045	1.9020	1.9010
	HSDT [5]	1.8937		
	Elasticity [36]	1.9540		
$\overline{\sigma}_{xx}$	Quadratic	0.6966	0.7009	0.7029
	Cubic	0.7074	0.7063	0.7061
	Quartic	0.7062	0.7060	0.7058
	HSDT [5]	0.6651		
	Elasticity [36]	0.7200		
$\overline{\sigma}_{yy}$	Quadratic	0.6179	0.6221	0.6239
	Cubic	0.6277	0.6270	0.6268
	Quartic	0.6268	0.6267	0.6266
	HSDT [5]	0.6322		
	Elasticity [36]	0.6660		
$\overline{\tau}_{xz}$	Quadratic	0.2293	0.2246	0.2227
	Cubic	0.2210	0.2205	0.2202
	Quartic	0.2205	0.2202	0.2201
	HSDT [5]	0.2064		
	Elasticity [36]	0.2700		

4.1.1 Four layer $(0°/90°)_s$ square cross-ply laminated plate under sinusoidal load

A square simply supported laminate of side length a and thickness h, composed of four equally thick layers oriented at $(0°/90°)_s$ is considered. The plate is subjected to a sinusoidal vertical pressure given by Equation (20). The material properties are as follows: $E_1 = 25E_2$; $G_{12} = G_{13} = 0.5E_2$; $G_{23} = 0.2E_2$; $\nu_{12} = 0.25$. For this example, a three-dimensional exact solution by Pagano [36] is available. The central deflection and the corresponding stresses for the SINUS-W2 theory with an isogeometric approach are shown in Table 2. We compare the results with higher order plate theories [5, 37], a first order theory [38], an exact solution [36] and also with the strain smoothing approach with SINUS-W2. The effect of the plate thickness is also shown in Table 2. It is shown clearly that the first order shear deformation theories (FSDT) cannot be used for thick laminates. Further, it can be seen that the results from the present formulation are in very good agreement with those in the literature and very precise transverse displacement and stress values are obtained.

4.1.2 Three layer (0°/90°/0°) square cross ply laminated plate under sinusoidal load

A square laminate of side a and thickness h, composed of three equally thick layers oriented at (0°/90°/0°) is considered. It is simply supported at all edges and subjected to a sinusoidal vertical pressure of the form given by Equation (20). The material properties for this example are: E_1 =132.38 GPa, $E_2 = E_3$ =10.756 GPa, G_{12} =3.606 GPa, $G_{13} = G_{23}$ = 5.6537 GPa, $\nu_{12} = \nu_{13}$ = 0.24, ν_{23} = 0.49. In Table 3, we present results for the SINUS-W2 theory with an isogeometric approach with quadratic, cubic and quartic NURBS basis functions having a 9×9 NURBS patch. The results from the present formulation are compared with the analytical solution [10, 39] and the MITC4 formulation with and without strain smoothing [22, 23]. It can be seen that the numerical results from the present formulation are in good agreement with the existing solutions. Moreover, it is noted that with the isogeometric approach, the geometry of the domain can be represented exactly. Although only a simple geometry is considered, the proposed formulation can easily be extended to complex geometies. The main features of the present formulation are: (1) theories from ESL to higher order layer descriptions can be implemented within a single program (since it is based on the CUF); (2) the isogeometric approach provides flexibility to construct higher order smooth functions and provides accurate solutions even for a coarse NURBS mesh and (3) the present formulation is insensitive to shear locking.

4.2 Free vibration - cross-ply laminated rectangular plates

Next, we study the fundamental frequencies of cross-ply laminated plates based on the proposed formulation. In this example, all layers of the laminate are assumed to be of the same thickness, density and made up of the same linear elastic material. The following material parameters are considered for each layer

$$\frac{E_1}{E_2} = 10,20,30, \text{ or } 40; \quad G_{12} = G_{13} = 0.6E_2; \quad G_3 = 0.5E_2; \nu_{12} = 0.25.$$

The subscripts 1 and 2 denote the directions normal and the transverse to the fibre direction in a lamina, which may be oriented at an angle with respect to the plate axes. The ply angle of each layer is measured from the global $x-$axis to the fibre direction. The example considered is a simply supported square cross-ply laminated plate$[0°/90°]_s$. The thickness and length of the plate are denoted by h and a, respectively. A thickness-to-span ratio of $h/a = 0.2$ is employed in the computations. In this study, we present the non-dimensionalized free flexural frequencies as:

$$\Omega = \omega \frac{a^2}{h} \sqrt{\frac{\rho}{E_2}}$$

unless specified otherwise. Table 4 shows the convergence of the normalized fundamental frequency of a simply supported cross-ply laminated square plate based on the current isogeometric approach. The performance of various basis functions with NURBS mesh refinement is studied. It can be seen that, as expected with $h-$ refinement, the solutions converge and with $p-$ refinement, the accuracy increases for the same mesh size. Table 5 lists the fundamental frequency for a simply supported cross-ply laminated square plate with $h/a = 0.2$ and for different Young's modulus ratios, E_1/E_2. It can be seen that the results from the present formulation are in very close agreement with the values reported in [41] based on higher order theory, the meshfree results of Liew *et al.*, [40] and Ferreira *et al.*, which are based on FSDT and higher order theories with radial basis functions [42]. The effect of plate thickness on the fundamental frequency is shown in Table 6. It can be seen that the results agree with the results available in the literature. The present formulation is insensitive to shear locking.

Table 2: The normalized central deflection $\overline{w} = w(a/2, a/2, 0)\frac{100E_2h^3}{Pa^4}$, stresses, $\overline{\sigma}_{xx} = \sigma_{xx}(a/2, a/2, h/2)\frac{h^2}{Pa^2}$, $\overline{\sigma}_{yy} = \sigma_{yy}(a/2, a/2, h/4)\frac{h^2}{Pa^2}$ and $\overline{\tau}_{xz} = \tau_{xz}(0, /a2, 0)\frac{h}{Pa}$ of a simply supported cross-ply laminated square plate [0°/90°/90°/0°], with $E_1 = 25E_2$, $G_{12} = G_{13} = 0.5E_2$, $G_{23} = 0.2E_2$, ν_{12} =0.25.

a/h	Method	w	σ_{xx}	σ_{yy}	τ_{xz}
	HSDT [5]	0.7147	0.5456	0.3888	0.2640
	FSDT [38]	0.6628	0.4989	0.3615	0.1667
10	Elasticity [36]	0.7430	0.5590	0.4030	0.3010
	RBF [37]	0.7325	0.5627	0.3908	0.3321
	CS-FEM Q4 (4 subcells) [23]	0.7195	0.5597	0.3905	0.2952
	Present (Quadratic 9× 9)	0.7250	0.5571	0.3908	0.2985
	Present (Cubic 9×9)	0.7203	0.5596	0.3913	0.2983
	Present (Quartic 9×9)	0.7187	0.5594	0.3907	0.2967
	HSDT [5]	0.4343	0.5387	0.2708	0.2897
	FSDT [38]	04337	0.5382	0.2705	0.1780
100	Elasticity [36]	0.4347	0.5390	0.2710	0.3390
	RBF [37]	0.4307	0.5431	0.2730	0.3768
	CS-FEM Q4 (4 subcells) [23]	0.4304	0.5368	-	0.3285
	Present (Quadratic 9× 9)	0.4383	0.5334	-	0.4069
	Present (Cubic 9×9)	0.4336	0.5368	-	0.3271
	Present (Quartic 9×9)	0.4317	0.5366	-	0.3275

Table 3: Transverse displacement $\overline{w} = w(a/2, a/2, h/2)$ at the center of a multilayered plate [0°/90°/0°] with E_1 = 132.38 GPa, $E_2 = E_3$ = 10.756 GPa, G_{12} = 3.606 GPa, $G_{13} = G_{23}$ = 5.6537 GPa, $\nu_{12} = \nu_{13} = 0.24$, $\nu_{23} = 0.49$.

$\overline{w}$	a/h				
	10	50	100	500	1000
Analytical (ESL-2) [10, 39]	0.9249	0.7767	0.7720	0.7705	0.7704
MITC4 [22]	0.9195	0.7713	0.7666	0.7650	0.7650
CS-FEM Q4 (4 subcells) [23]	0.9235	0.7703	0.7655	0.7639	0.7639
Present (Quadratic 9×9)	0.9252	0.7713	0.7650	0.7624	0.7624
Present (Cubic 9×9)	0.9226	0.7704	0.7656	0.7640	0.7639
Present (Quartic 9×9)	0.9217	0.7695	0.7646	0.7631	0.7630

Table 4: Convergence of the normalized fundamental frequency $\Omega = \omega a^2/h\sqrt{\rho/E_2}$ of a simply supported cross-ply laminated square plate $(0°/90°)_s$ with $h/a = 0.2$, $\frac{E_1}{E_2} = 40$, $G_{12} = G_{13} = 0.6E_2$, $G_{23} = 0.5E_2$, $\nu_{12} = 0.25$..

Method	Meshes		
	5×5	7× 7	9×9
Quadratic	10.6926	10.7295	10.7454
Cubic	10.7340	10.7517	10.7590
Quartic	10.7498	10.7598	10.7640

4.3 Free vibration - cross-ply laminated circular plates

In this example, consider a circular four layer $[\theta/-\theta/-\theta/\theta]$ laminated plate with fully clamped boundary conditions. The influence of the fiber orientations on the free vibration of a clamped circular laminated plate is studied. The following material properties are used:

$$\frac{E_1}{E_2} = 40; \quad G_{12} = G_{13} = 0.6E_2;$$
$$G_3 = 0.5E_2; \nu_{12} = 0.25.$$

The subscripts 1 and 2 denote the directions normal and the transverse to the fibre direction in a lamina. The circular plate has a radius-to-thickness ratio of 5 (R/h =5). For this problem, a NURBS quadratic basis function is sufficiently accurate to model the circular geometry. Any

Table 5: The normalized fundamental frequency $\Omega = \omega a^2/h\sqrt{\rho/E_2}$ of a simply supported cross-ply laminated square plate $(0°/90°)_s$ with $h/a = 0.2$, $\frac{E_1}{E_2}$ = 10, 20, 30 or 40, $G_{12} = G_{13} = 0.6E_2$, $G_{23} = 0.5E_2$, $\nu_{12} = 0.25$.

Method	E_1/E_2			
	10	20	30	40
Liew [40]	8.2924	9.5613	10.3200	10.8490
Reddy, Khdeir [41]	8.2982	9.5671	10.3260	10.8540
HSDT [42] ($\nu_{23} = 0.18$)	8.2999	9.5411	10.2687	10.7652
CS-FEM Q4 (4 subcells) [23]	8.3642	9.5793	10.2973	10.7887
Present (Quadratic 9×9)	8.3358	9.5437	10.2572	10.7454
Present (Cubic 9×9)	8.3417	9.5532	10.2691	10.7590
Present (Quartic 9×9)	8.3439	9.5566	10.2734	10.7640

Table 6: Variation of fundamental frequencies, $\Omega = \omega a^2/h\sqrt{\rho/E_2}$ with a/h for a simply supported square laminated plate $[0°/90°/90°/0°]$, $\Omega = \omega a^2/h\sqrt{\rho/E_2}$, with $E_1/E_2 = 40$, $G_{12} = G_{13} = 0.6E_2$, $G_{23} = 0.5E_2$, $\nu_{12} = \nu_{13} = \nu_{23} = 0.25$.

Method	a/h					
	2	4	10	20	50	100
FSDT [43]	5.4998	9.3949	15.1426	17.6596	18.6742	18.8362
Model-1 (12dofs) [9]	5.4033	9.2870	15.1048	17.6470	18.6720	18.8357
Model-2 (9dofs) [9]	5.3929	9.2710	15.0949	17.6434	18.6713	18.8355
HSDT [5]	5.5065	9.3235	15.1073	17.6457	18.6718	18.8356
HSDT [44]	6.0017	10.2032	15.9405	17.9938	18.7381	18.8526
CS-FEM Q4 (4 subcells) [23]	5.4026	9.2998	15.1766	17.7540	18.7947	18.9611
Present (Quadratic 9×9)	5.3931	9.2701	15.0660	17.5781	18.5913	18.7579
Present (Cubic 9×9)	5.3945	9.2785	15.1086	17.649	18.6711	18.8343
Present (Quartic 9×9)	5.3951	9.2815	15.1239	17.6749	18.7024	18.8665

further refinement, would will only improve the accuracy of the solution. The following knot vectors for the coarsest mesh with one element are defined as follows: Ξ =[0,0,0,1,1,1]; and $\mathcal{H}$ =[0,0,0,1,1,1]. The parameters for the circular plate is given in Table 7. In this study, 13×13 NURBS cubic elements are used. The first three fundamental frequencies for a clamped circular laminated plate are given in Table 8. The fibre orientation of each layer is considered to be the same, and the influence of the fibre orientation on the first three fundamental frequencies is given in Table 8. The numerical results from the present approach are compared with the moving least square differential quadrature method (MLSDQ), which is based on FSDT [40] and IGA with inverse trigonometric shear deformation theory [45]. It can be seen that the results from the present formulation agree well with the results in the literature.

Table 7: Control points and weights for a circular plate with radius $R = 0.5$.

i	1	2	3	4	5	6	7	8	9
x_i	$-\frac{\sqrt{2}}{4}$	$-\frac{\sqrt{2}}{2}$	$\frac{\sqrt{2}}{4}$	0	0	0	$\frac{\sqrt{2}}{4}$	$\frac{\sqrt{2}}{2}$	$\frac{\sqrt{2}}{4}$
y_i	$\frac{\sqrt{2}}{4}$	0	$-\frac{\sqrt{2}}{4}$	$\frac{\sqrt{2}}{2}$	0	$-\frac{\sqrt{2}}{2}$	$\frac{\sqrt{2}}{4}$	0	$-\frac{\sqrt{2}}{4}$
w_i	1	$\frac{\sqrt{2}}{2}$	1	$\frac{\sqrt{2}}{2}$	1	$\frac{\sqrt{2}}{2}$	1	$\frac{\sqrt{2}}{2}$	1

5 Conclusions

In this article, the isogeometric approach was combined with the unified formulation to study the static bending and the free vibration of laminated composites. The present approach allows us to achieve a smooth approximation of the unknown fields with arbitrary continuity. When employing lower order elements, the method suffers from the shear locking syndrome, which is alleviated by multiplying the shear term with a correction factor. The results from the present formulation are in very good agreement with the solutions available in the literature. We believe that the present formulation is an effective compu-

Table 8: Influence of fiber orientations on the fundamental frequencies, $\Omega = \omega a^2/h\sqrt{\rho/E_2}$ for clamped circular laminated plates.

θ	Method	Ω		
		1	2	3
0	MLSDQ-FSDT [40]	22.2110	29.651	41.1010
	IGA [45]	23.5781	30.7459	42.0042
	Present	22.6663	30.3485	41.7294
$\pi/12$	MLSDQ-FSDT [40]	22.7740	31.4550	43.350
	IGA [45]	23.6090	31.7743	43.9569
	Present	23.0024	31.5752	43.7671
$\pi/6$	MLSDQ-FSDT [40]	24.0710	36.1530	43.9680
	IGA [45]	24.2081	35.6047	46.5406
	Present	23.9749	35.2577	44.2964
$\pi/4$	MLSDQ-FSDT [40]	24.7520	39.1810	43.6070
	IGA [45]	24.6607	37.8980	46.2560
	Present	24.5253	37.4311	44.0796

tational formulation for practical problems. On one hand, the unified formulation allows the user to test different theories within a single framework, and the isogeometric approach provides flexibility in constructing higher-order smooth basis functions, and the geometry is accurately described.

References

[1] H. Man, C. Song, T. Xiang, W. Gao, F. Tin-Loi, High-order plate bending analysis based on the scaled boundary finite element method, International Journal for Numerical Methods in Engineering 95 (2013) 331–360.

[2] T. Xiang, S. Natarajan, H. Man, C. Song, W. Gao, Free vibration and mechanical buckling of plates with in-plane material inhomogeneity - a three dimensional consistent approach, Composite Structures.

[3] R. Khandan, S. Noroozi, P. Sewell, J. Vinney, The development of laminated composite plate theories: a review, J. Mater. Sci. 47 (2012) 5901–5910.

[4] Mallikarjuna, T. Kant, A critical review and some results of recently developed refined theories of fibre reinforced laminated composites and sandwiches, Composite Structures 23 (1993) 293–312.

[5] J. Reddy, A simple higher order theory for laminated composite plates, ASME J Appl Mech 51 (1984) 745–752.

[6] Y. Guo, A. P. Nagy, Z. Gürdal, A layerwise theory for laminated composites in the framework of isogeometric analysis, Composite Structures 107 (2014) 447–457.

[7] L. Demasi, ∞^6 Mixed plate theories based on the Generalized Unified Formulation Part I: Governing equations, Composite Structures 87 (2009) 1–11.

[8] R. Rolfes, K. Rohwer, Improved transverse shear stresses in composite finite elements based on first order shear formation theory, International Journal for Numerical Methods in Engineering 40 (1997) 51–60.

[9] T. Kant, K. Swaminathan, Analytical solutions for free vibration of laminated composite and sandwich plates based on a higher-order refined theory, Composite Structures 53 (1) (2001) 73–85.

[10] E. Carrera, Developments, ideas and evaluations based upon the Reissner's mixed variational theorem in the modelling of multilayered plates and shells, Appl. Mech. Rev. 54 (2001) 301–329.

[11] E. Carrera, L. Demasi, Classical and advanced multilayered plate elements based upon PVD and RMVT. Part 1: derivation of finite element matrices, International Journal for Numerical Methods in Engineering 55 (2002) 191–231.

[12] A. Ferreira, E. Viola, F. Tornabene, N. Fantuzzi, A. Zenkour, Analysis of sandwich plates by generalized differential quadrature method, Mathematical Problems in Engineering 964367 (2013) 1–12.

[13] A. Ferreira, E. Carrera, M. Cinefra, E. Viola, F. Tornabene, N. Fantuzzi, A. Zenkour, Analysis of thick isotropic and cross-ply laminated plates by generalized differential quadrature method and a unified formulation, Composite Part B: Engineering 58 (2014) 544–552.

[14] C. Shu, W. Wu, H. Ding, C. Wang, Free vibration analysis of plates using least-square finite difference method, Computer Methods in Applied Mechanics and Engineering 196 (2007) 1330–1343.

[15] O. Civalek, B. Ozturk, Vibration analysis of plates with curvilinear quadrilateral domains by discrete singular convolution method, Structural Engineering and Mechanics 36 (2010) 279–299.

[16] M. Ganapathi, O. Polit, M. Touratier, A $\mathcal{C}^o$ eight-node membrane-shear-bending element for geometrically nonlinear (static and dynamic) analysis of laminates, International Journal for Numerical Methods in Engineering 39 (1996) 3453–3474.

[17] H. Kapoor, R. Kapania, Geometrically nonlinear NURBS isogeometric finite element analysis of laminated composite plates, Composite Structures 94 (2012) 3434–3447.

[18] T. Q. Bui, M. N. Nguyen, C. Zhang, An efficient meshfree method for vibration analysis of laminated composite plates, Computational Mechanics 48 (2011) 175–193.

[19] K. Liew, X. Zhao, A. J. Ferreira, A review of meshless methods for laminated and functionally graded plates and shells, Composite

Structures 93 (2011) 2031–2041.
[20] Y. Xing, B. Liu, High-accuracy differential quadrature finite element method and its application to free vibration of thin plate with curvilinear domain, International Journal for Numerical Methods in Engineering 80 (2009) 1718–1742.
[21] X. Wang, Y. Wang, Z. Yuan, Accurate vibration analysis of skew plates by the new version of the differential quadrature method, Applied Mathematical Modelling 38 (2014) 926–937.
[22] E. Carrera, M. Cinefra, P. Nali, MITC technique extended to variable kinematic multilayered plate elements, Composite Structures 92 (2010) 1888–1895.
[23] S. Natarajan, A. Ferreira, S. Bordas, E. Carrera, M. Cinefra, Analysis of composite plates by a unified formulation-cell based smoothed finite element method and field consistent elements, Composite Structures 105 (2013) 75–81.
[24] T. Hughes, M. Cohen, M. Haroun, Reduced and selective integration techniques in finite element method of plates, Nuclear Engineering Design 46 (1978) 203–222.
[25] H. Nguyen-Xuan, T. Rabczuk, S. Bordas, J. Debongnie, A smoothed finite element method for plate analysis, Computer Methods in Applied Mechanics and Engineering 197 (2008) 1184–1203.
[26] B. R. Somashekar, G. Prathap, C. R. Babu, A field-consistent four-noded laminated anisotropic plate/shell element, Computers and Structures 25 (1987) 345–353.
[27] K. Bathe, E. Dvorkin, A four-node plate bending element based on Mindlin/Reissner plate theory and a mixed interpolation, International Journal for Numerical Methods in Engineering 21 (1985) 367–383.
[28] H. Santos, J. Evans, T. Hughes, Generalization of the twist-Kirchhoff theory of plate elements to arbitrary quadrilaterals and assessment of convergence, Computer Methods in Applied Mechanics and Engineering 209–212 (2012) 101–114.
[29] C. H. Thai, H. Nguyen-Xuan, N. Nguyen-Thanh, T.-H. Le, T. Nguyen-Thoi, T. Rabczuk, Static, free vibration, and buckling analysis of laminated composite Reissner-Mindlin plates using NURBS-based isogeometric approach, International Journal for Numerical Methods in Engineering 91 (2012) 571–603.
[30] L. de Veiga, A. Buffa, C. Lovadina, M. Martinelli, G. Sangalli, An isogeometric method for the Reissner-Mindlin plate bending problem, Computer Methods in Applied Mechanics and Engineering 45–53 (2012) 209–212.
[31] E. Carrera, L. Demasi, Classical and advanced multilayered plate elements based upon PVD and RMVT. Part 2: Numerical implementations, International Journal for Numerical Methods in Engineering 55 (2002) 253–291.
[32] J. Cottrell, T. Hughes, Y. Bazilevs, Isogeometric analysis: toward integration of CAD and FEA, John Wiley, 2009.
[33] N. Valizadeh, S. Natarajan, O. A. Gonzalez-Estrada, T. Rabczuk, T. Q. Bui, S. P. Bordas, NURBS-based finite element analysis of functionally graded elastic plates: Static bending, vibration, buckling and flutter, Composite Structures 99 (2013) 309–326.
[34] F. Kikuchi, K. Ishii, An improved 4-node quadrilateral plate bending element of the Reissner-Mindlin type, Compuational Mechanics 23 (1999) 240–249.
[35] M. Touratier, An efficient standard plate theory, International Journal of Engineering Science 29 (1991) 901–916.
[36] N. Pagano, Exact solutions for rectangular bidirectional composites and sandwich plates, Journal of Composite Materials 4 (1970) 20–34.
[37] A. Ferreira, E. Carrera, M. Cinefra, C. Roque, Radial basis functions collocation for the bending and free vibration analysis of laminated plates using the Reissner-Mixed variational theorem, European Journal of Mechanics - A/Solids 39 (2012) 104–112.
[38] J. Reddy, W. Chao, A comparison of closed-form and finite-element solutions of thick laminated anisotropic rectangular plates, Nuclear Engineering and Design 64 (1981) 153–167.
[39] E. Carrera, Evaluation of layer-wise mixed theories for laminated plates analysis, AIAA J 26 (1998) 830–839.
[40] K. Liew, Y. Huang, J. Reddy, Vibration analysis of symmetrically laminated plates based on FSDT using the moving least squares differential quadrature, Computer Methods in Applied Mechanics and Engineering 192 (2003) 2203–2222.
[41] A. Khdeir, L. Librescu, Analysis of symmetric cross-ply elastic plates using a higher-order theory: Part II: buckling and free vibration, Composite Structures 9 (1988) 259–277.
[42] A. Ferreira, C. Roque, E. Carrera, M. Cinefra, Analysis of thick isotropic and cross-ply laminated plates by radial basis functions and a unified formulation, Journal of Sound and Vibration 330 (2011) 771–787.
[43] J. Whitney, N. Pagano, Shear deformation in heterogeneous anisotropic plates, ASME J Appl Mech 37 (4) (1970) 1031–1036.
[44] N. Senthilnathan, K. Lim, K. Lee, S. Chow, Buckling of shear deformable plates, AIAA J 25 (9) (1987) 1268–1271.
[45] C. H. Thai, A. Ferreira, S. Bordas, T. Rabczuk, H. Nguyen-Xuan, Isogeometric analysis of laminated composite and sandwich plates using a new inverse trigonometric shear deformation theory, European Journal of Mechanics - A/Solids 43 (2014) 89–108.